Trans Indian Inst Met (2016) 69(2):325–329
DOI 10.1007/s12666-015-0784-5

TECHNICAL PAPER

Strain Amplitude and Temperature Effects on the Low Cycle Fatigue Behavior of Alloy 617M

K. Mariappan[1] · Vani Shankar[1] · Sunil Goyal[1] · R. Sandhya[1] · K. Laha[1] · A. K. Bhaduri[1]

Received: 9 October 2015 / Accepted: 17 November 2015 / Published online: 19 December 2015

Abstract In the present investigation, comparative evaluation of the low cycle fatigue (LCF) of tube and forged Alloy 617M have been studied. Total axial strain controlled tests were performed on sub-sized specimens between 300 and 1023 K employing strain amplitudes ranging from ± 0.25 to ± 1 % at a nominal strain rate of 3×10^{-3} s^{-1}. The alloy underwent cyclic hardening at all temperatures and strain amplitudes and the rate of hardening was sensitive to both temperature and strain amplitude. There were distinct differences in the LCF behavior of forged and tube products. The forged alloy exhibited better fatigue life than that of tube material and significant difference in the rate of hardening was observed between the material conditions at 1023 K. The variation in the LCF behavior of the two products was found to be associated with the difference in the initial microstructure. The grains of the tube product were equiaxed having 214 μm average size whereas a distribution of both large grains (average 65 μm) and clusters of small grains (average 15 μm) were found in the forged product. Microstructural investigations revealed mixed mode of failure for both the product forms.

Keywords LCF · Alloy 617M · Strain amplitude · Temperature · CSR · Microstructure

✉ K. Mariappan
mariappan@igcar.gov.in

[1] Materials Development and Technology Group, Indira Gandhi Centre for Atomic Research, Kalpakkam 603102, India

1 Introduction

This study was performed as a part of the comprehensive materials testing program of India's national mission for the development of advanced high temperature materials, manufacturing technologies and design of equipments for a 800 MW demonstration advanced ultra supercritical (AUSC) power plant [1]. The nickel base Alloy 617M, a modified version of Alloy 617 [2], has been identified as the candidate material for boiler and turbine components of AUSC power plants. System start-ups and shut-downs as well as power transients will produce LCF loadings of components [3]. Though the documentation on the LCF properties of nickel base superalloys have been made at higher temperatures [3–6], it is also necessary to characterize the fatigue behavior of these alloys under the start-up condition at room temperature and at intermediate temperatures. Therefore, the present work aims to examine the influence of different strain amplitudes and temperatures, particularly intermediate temperatures, on cyclic stress response and fatigue lives of tube and forged products of Alloy 617M.

2 Experimental

The material was obtained as extruded tube and forged block in the mill solution annealed condition. The chemical composition of the extruded tube and the forged product of Alloy 617M is given in Table 1. The uniform-gauge test sections of the specimens were 6 mm in diameter 15 mm in length. Fully reversed strain-controlled low cycle fatigue experiments were carried out in a DARTEC servo-hydraulic system in-built with a electrical resistance furnace. The tests were conducted at various strain amplitudes of

Table 1 Chemical composition of Alloy 617M tube (T) and forged (F) material

Element	C	Mo	Fe	Co	Ti	Cr	Si	Al	Ni
wt% (T)	0.06	9.26	0.15	12.09	0.41	22.19	0.05	1.12	Bal.
wt% (F)	0.07	9.1	0.12	11.6	0.4	22.1	0.02	1.2	Bal.

±0.25, ±0.4, ±0.6 and ±1.0 % and at temperatures of 300, 923, 973 and 1023 K, at a nominal strain rate of 3×10^{-3} s^{-1}. The temperature fluctuation was maintained within ±2 K over the gauge length. LCF testing was conducted in accordance with ASTM standard E606 [7]. Optical and scanning electron microscopy were carried out to assess the changes in the microstructure during cyclic loading. Etching for optical microscopy was done on the polished surface of the untested and tested samples using Nital etchant with the composition of 90 % methanol and 10 % nitric acid.

3 Results and Discussion

3.1 Initial Microstructure and Cyclic Stress Response

The optical micrographs of tube and forged forms of Alloy 617M are shown in Fig. 1a, b respectively. The initial microstructure of the alloy tube material consists of well defined austenite grain boundaries with average equiaxed grains (size 214 μm) whereas the forged material showed a distribution of both large grains (size average 65 μm) and clusters of small grains (size average 15 μm). The average grain diameter was calculated by linear intercept method. Both the materials revealed the presence of annealed twin boundaries.

The influences of strain amplitude and temperature on cyclic stress response (CSR) of the tube product of the alloy are depicted in Fig. 2a–c. For comparison, the CSR of forged material is shown in Fig. 2c. Cyclic stress response curves were constructed by picking up the peak tensile stress value for the corresponding cycle number. In both the product forms, the material exhibited initial cyclic hardening followed by saturation or softening (depending on the strain amplitude and temperature) and sudden drop in load due to the macro crack development and finally failure. The Fig. 2a–c make it clear that the CSR behavior of this alloy is strongly dependent on the imposed total strain, temperature and the product form.

Irrespective of temperature, with an increase in strain amplitude there was an overall increase in CSR for both the products of the alloy as shown in Fig. 2a, c. At room temperature, cyclic hardening in the initial cycles followed by softening was observed except for lower strain amplitudes. At the lower strain amplitude (±0.25 %) there was slow rise in stress response and a saturation phase. Increase in the amount of hardening and softening with the increase in strain amplitude as observed in the present study (Fig. 2a) has been reported earlier by other researchers [8–10]. The cyclic hardening in the initial cycles is due to the dislocation multiplication and accumulation within the slip band [9]. The higher softening rate with increase in strain amplitude, at the room temperature, may be attributed to the formation of micro-twins which will contribute to most

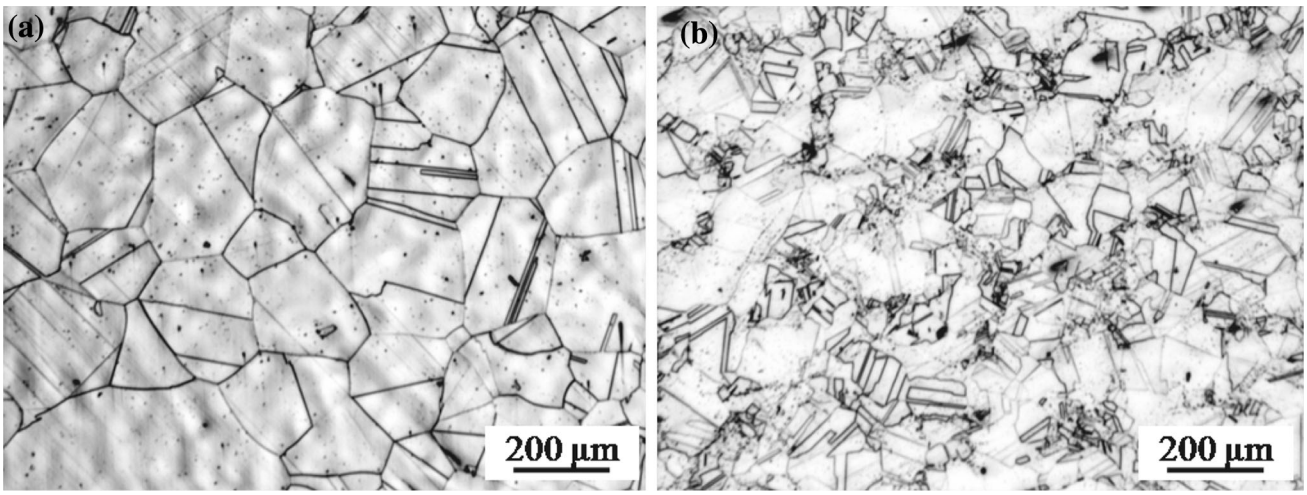

Fig. 1 Initial microstructures of tube (**a**) and forged (**b**) forms of Alloy 617M

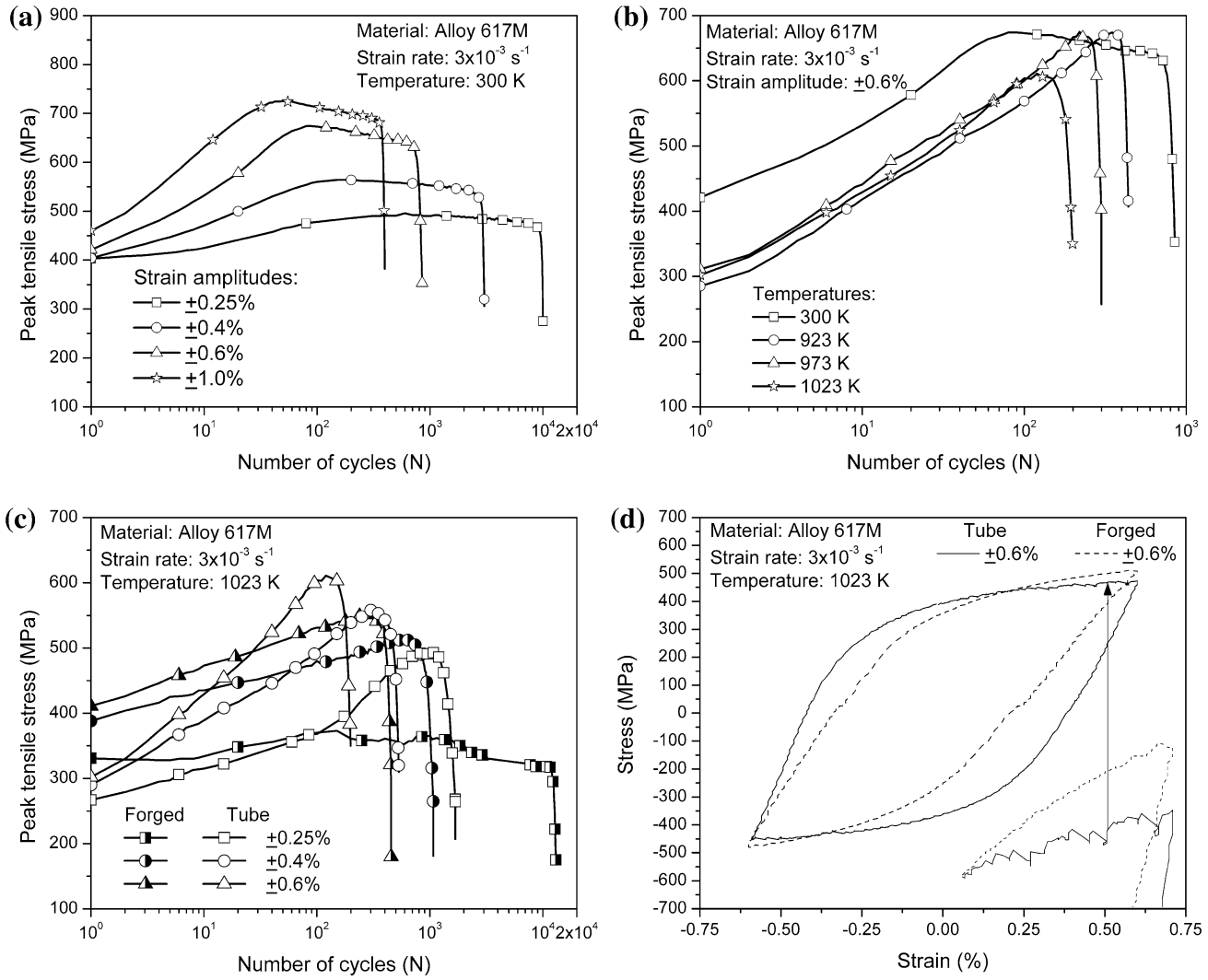

Fig. 2 Effects of strain amplitude in tube material (**a**), temperature, in tube material (**b**) and product forms (**c**) on cyclic stress response of Alloy 617M. Representative hysteresis loop for serrated flow characteristic (**d**)

of the localized deformation and annihilation of dislocations due to increasing in dislocation density with cycling also takes place [9]. With the increase in temperature, the overall CSR of the tube form shifts downwards and falls within a narrow band as shown in Fig. 2b. The material shows continuous steep cyclic hardening at all the higher test temperatures. The hysteresis loops show serrations (Fig. 2d) which is one of the manifestations of the occurrence of the dynamic strain aging (DSA) [11]. Therefore the typical steep cyclic hardening behavior of this material in the temperature range 923–1023 K may be attributed to the DSA.

At elevated temperature, 1023 K, the two products (tube and forged) display a difference in the cyclic hardening behavior as shown in Fig. 2c. The tube product of the alloy showed gradual cyclic hardening followed by steep secondary cyclic hardening whereas forged material showed almost saturation in the stress response from the first cycle onwards at lower strain amplitude. The secondary cyclic hardening has been observed at lower strain amplitude at low temperature (477 K) by Chai et al. [9]. According to Chai et al. [9] the secondary hardening is ascribed to the interaction between the stacking faults and the moving dislocation. At higher strain amplitudes both the product forms of alloy exhibited more or less continuous cyclic hardening followed by drop in stress to final failure. Burke et al. [12] have observed similar results at 1033 K for this alloy. The continuous cyclic hardening was attributed to the formation of dislocation substructure which provides sites for numerous heterogeneous precipitations of fine $M_{23}C_6$ particles, which in turn, stabilizes the substructure during further cycling, preventing the recovery processes [12]. Precipitation analysis was not carried out in this study.

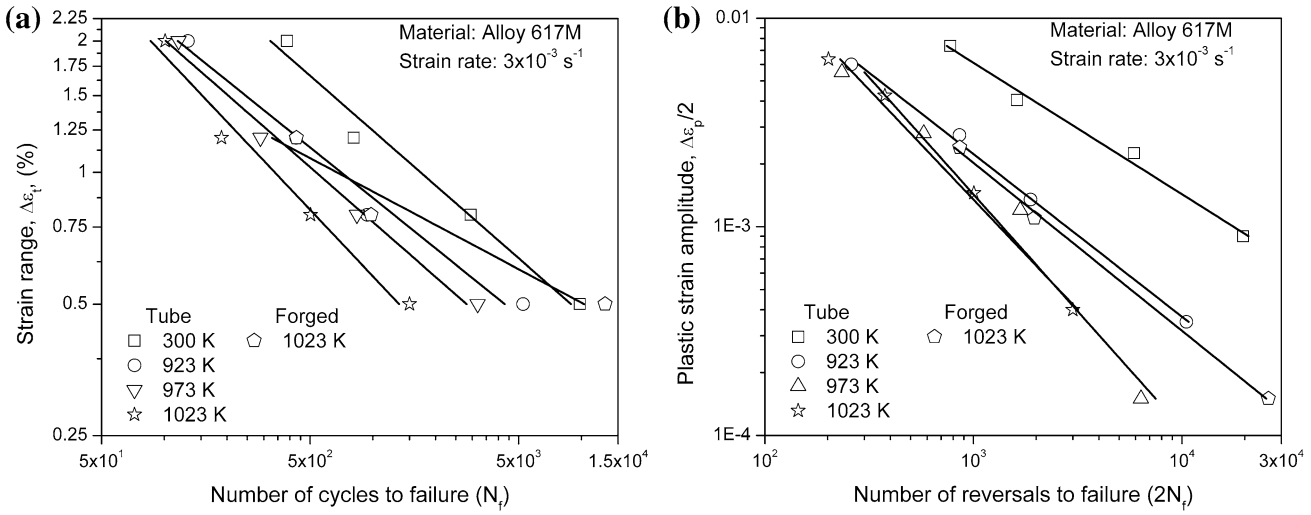

Fig. 3 Strain-life (**a**) and Coffin-Manson (**b**) plots of Alloy 617M

3.2 Fatigue Life

Total strain range ($\Delta\varepsilon_t$, %) versus cycles to failure (N_f) and half-life plastic strain amplitude ($\Delta\varepsilon_p/2$) versus number of reversals to failure ($2N_f$) are plotted on log–log scale for both tube and forged products of the alloy (Fig. 3a, b respectively). From Fig. 3a it is clear that the fatigue life decreases with increase in strain amplitude and temperature. Further it is observed that the fatigue life is inversely proportional to plastic strain experienced by this alloy (Fig. 3b). The forged product showed higher fatigue resistance than the tube product of the alloy at all strain amplitudes and at 1023 K. As has been mentioned earlier larger grains were observed for the tube product whereas the forged form had shown clusters of small grains (Fig. 1). Hence one possible reason for life improvement in forged form is the presence of fine grains [4]. It is clear from the half life hysteresis loop (Fig. 2d) that the loop area for the forged product is much lower as compared to tube product at 1023 K. The plastic strain accumulated depicts (Fig. 3b) the permanent deformation accumulated that causes the damage in the material. Therefore it may be concluded that the grain refinement and lower plastic strain accumulation in the forged product improve the fatigue life.

3.3 Optical and Scanning Electron Microscopy

Representative optical micrographs of polished and etched tube and forged material specimens taken from normal to the fracture surface revealed significant microstructural development as shown in Fig. 4a, b respectively. Qualitatively, the length and number of secondary cracks increases with the strain amplitude and temperature (not shown).

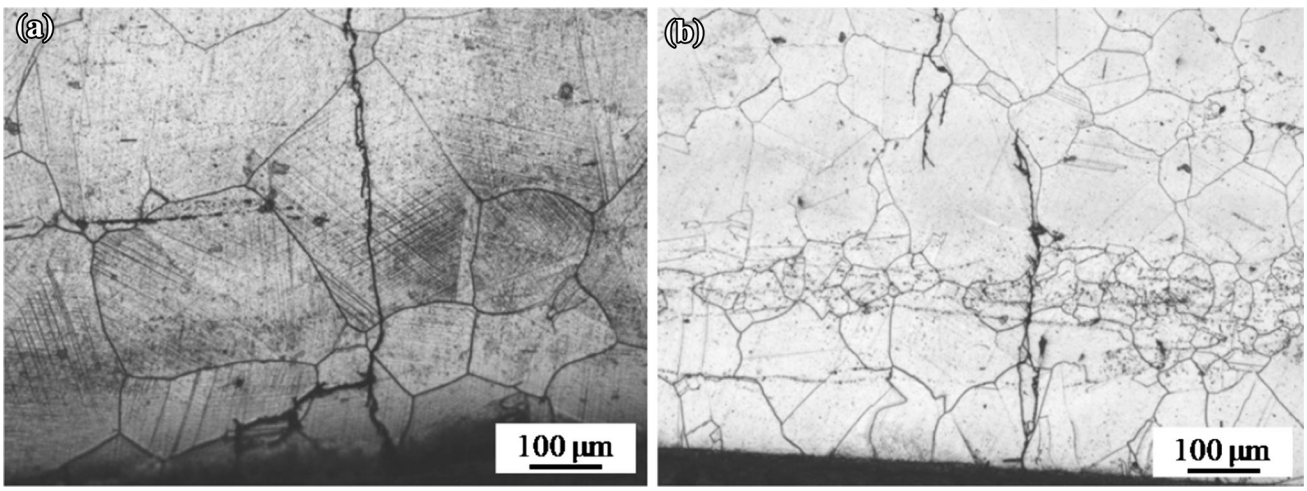

Fig. 4 Comparison of formation of secondary cracks in the tube (**a**) and forged (**b**) products of Alloy 617M LCF tested at ±0.4 % and 1023 K

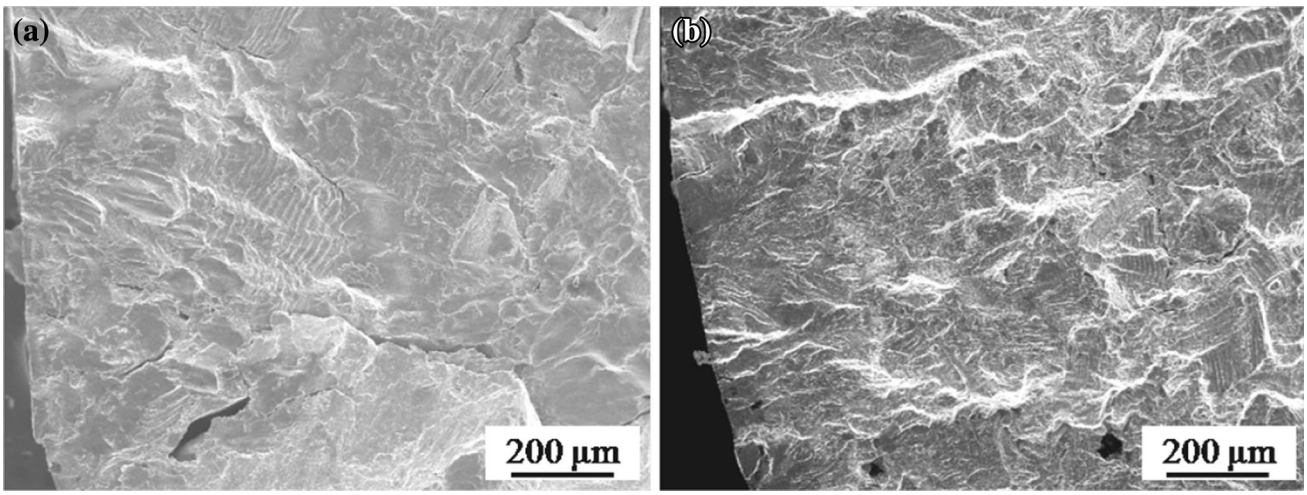

Fig. 5 Fractographs of tube (**a**) and forged (**b**) forms of Alloy 617M LCF tested at ±0.6 % and 1023 K

As can be seen from Fig. 4a secondary crack has propagated continuously in the tube material. On the other hand, the crack propagation is hardly extended beyond the fine grain region of forged material which is clearly seen in the Fig. 4b. The arrest of the crack in the fine grains band could be the reason for the delay of the crack propagation which in turn results the improvement in fatigue life of forged material.

The fracture surfaces of the tube and forged forms of the alloy are shown in Fig. 5. Radial ridges and striations, and many intergranular facets are also in evidence. This is an indicative of a mixed-mode type of fracture.

4 Summary and Conclusions

Low cycle fatigue behavior of tube and forged forms of Alloy 617M has been characterized at various strain amplitudes and temperatures. Both the materials showed increase in fatigue life with decreasing strain amplitudes and test temperatures. Occurrence of dynamic strain aging causes the steep cyclic hardening behavior of the tube material at higher test temperatures. The improvement in fatigue life of forged material may be attributed to the arrest of crack propagation in the fine grain region of the material. Mixed mode of fracture is observed in both the materials.

References

1. Alok M, Bhutani O P, Jayakumar T, Dubey D K, and Chetal S C, in Proceedings of Seventh International Conference on Advances in Materials Technology for Fossil Power plants, Electric Power Research Institute, USA (2013) p 53.
2. ASME, Boiler and Pressure Vessel Code, Part B, SB-166 and 167 (2013) p 207.
3. Bhanu Sankara Rao K, Schiffers H, Schuster H, and Nickel H, *Met Trans A* **19** (1988) p 359.
4. Srivastava S K, and Klarstrom O L, in Proceedings of Conference on Gas Turbines, ASME (1990) 90-GT-80.
5. Wright J K, Carroll L J, Simpson J A, and Wright R N, *J Eng Mater Technol* **135** (2013) p 031005-1.
6. Maier G, Riedel H, and Somsen C, *Int J Fatigue* **55** (2013) p 126.
7. ASTM Designation E 606-80, Part 10 (1980) p 694.
8. Kim S J, Choi P H, Dewa R T, Kim W G, and Kim M H, *Proc Mater Sci* **3** (2014) p 2201.
9. Chai G, Liu P, and Frodigh J, *J Mater Sci* **39** (2004) p 2689.
10. Guo X G, Guo J T, Yuan C, and Yang H C, in Proceedings of the Eighth Liege Conference on Materials for Advanced Power Engineering (2006) p 403.
11. Cornet C, Wackermann K, Stocker C, Christ H -J, Lupton C, Hardy M, and Tong J, *Mater High Temp* **31** (2014) p 226.
12. Burke M A, and Beck C G, *Met Trans A* **15** (1984) p 661.